

BRNO UNIVERSITY OF TECHNOLOGY

Faculty of Mechanical Engineering

MASTER'S THESIS

Brno, 2025

Patrick Chequeller, BSC.



# BRNO UNIVERSITY OF TECHNOLOGY

VYSOKÉ UČENÍ TECHNICKÉ V BRNĚ

## FACULTY OF MECHANICAL ENGINEERING

FAKULTA STROJNÍHO INŽENÝRSTVÍ

## INSTITUTE OF AUTOMOTIVE ENGINEERING

ÚSTAV AUTOMOBILNÍHO A DOPRAVNÍHO INŽENÝRSTVÍ

# ADVANCED FUEL CELL MATHEMATICAL MODEL MODELLED IN MATLAB

POKROČILÝ MATEMATICKÝ MODEL PALIVOVÉHO ČLÁNKU MODELOVANÝ V PROSTŘEDÍ MATLAB

## MASTER'S THESIS

DIPLOMOVÁ PRÁCE

## AUTHOR

AUTOR PRÁCE

Patrick Chequeller, BSC.

## SUPERVISOR

VEDOUCÍ PRÁCE

Ing. Michael Böhm, Ph.D.

BRNO 2025



# Assignment Master's Thesis

Institut: Institute of Automotive Engineering  
Student: **Patrick Chequeller, BSC.**  
Degree program: Mechanical Engineering  
Branch: no specialisation  
Supervisor: **Ing. Michael Böhm, Ph.D.**  
Academic year: 2024/25

As provided for by the Act No. 111/98 Coll. on higher education institutions and the BUT Study and Examination Regulations, the director of the Institute hereby assigns the following topic of Master's Thesis:

## Advanced fuel cell mathematical model modelled in Matlab

### Brief Description:

Computational simulation work aimed at creating a mathematical model of a fuel cell incorporating all physical principles adequate for a given resolution level.

### Master's Thesis goals:

The main objective of the work is to create a mathematical model of the fuel cell in the Matlab/Simulink software environment.

Sub-objectives

Research on fuel cells (types, designs, etc.)

Mathematical/analytical description of physical phenomena in a fuel cell

Development of a mathematical model of the fuel cell

### Recommended bibliography:

Liu, X., Reddi, K., Elgowainy, A., Lohse-Busch, H., Wang, M., & Rustagi, N. (2020). Comparison of well-to-wheels energy use and emissions of a hydrogen fuel cell electric vehicle relative to a conventional gasoline-powered internal combustion engine vehicle. *International Journal of Hydrogen Energy*, 45(1), 972-983. <https://doi.org/10.1016/j.ijhydene.2019.10.192>.

Acar, C., & Dincer, I. (2020). The potential role of hydrogen as a sustainable transportation fuel to combat global warming. *International Journal of Hydrogen Energy*, 45(5), 3396-3406. <https://doi.org/10.1016/j.ijhydene.2018.10.149>.

Verhelst, S., & Wallner, T. (2009). Hydrogen-fueled internal combustion engines. *Progress in Energy and Combustion Science*, 35(6), 490-527. <https://doi.org/10.1016/j.pecs.2009.08.001>.

Deadline for submission Master's Thesis is given by the Schedule of the Academic year 2024/25

In Brno,

L. S.

---

prof. Ing. Josef Štětina, Ph.D.  
Director of the Institute

---

doc. Ing. Jiří Hlinka, Ph.D.  
FME dean

## **ABSTRACT**

This thesis presents a zero-dimensional proton exchange membrane fuel cell (PEMFC) model tailored for control-oriented and system-level simulations. The boundary conditions were considered on the stack inlets and the key parameters such as membrane resistance, exchange current density, and reactant flow rates were calibrated against published data, and a single-parameter least-squares tuning coefficient was applied to align the model's voltage-current characteristics with a benchmark, yielding a Mean Absolute Error of 0.6767 V and a Mean Relative Error of 1.45 %. Stack power and efficiency curves were analyzed across the current sweep, including visualizations of voltage, current, and power, demonstrating numerical stability and predictive accuracy. The results confirm that the integrated thermal, electrochemical, mass-transport, and hydration dynamics produce a robust tool for preliminary PEMFC design and control studies. Future work will involve validating the model's predictions against detailed experimental polarization, transient, thermal management, and hydration data to further refine parameters and support real-world hardware integration.

### **Key words**

PEM fuel cell, zero-dimensional model, membrane hydration, overpotential, control-oriented simulation.

## **DECLARATION OF AUTHENTICITY**

I hereby declare that I wrote my master's thesis ADVANCED FUEL CELL MATHEMATICAL MODEL MODELLED IN MATLAB independently and without outside assistance. I did not use any other sources apart from the ones stated in the bibliography and that I have clearly cited all passages (including graphics, tables, etc.) in the thesis that were taken from other sources. This thesis has never been submitted in its current or similar form in any other degree programme

23. 05. 2025

-----  
Date

-----  
*Patrick Chequeller*

## Table of contents

Introduction .....	8
1 The energy sector, environmental challenges and the role of fuel cells .....	10
1.1 Climate and energy system demands.....	10
1.2 Hydrogen and fuel cells in energy transition.....	11
2 Fuel cell principles .....	13
2.1 Polymer Electrolyte Membrane Fuel Cells .....	13
2.2 Review of PEMFC modelling .....	14
2.2.1 Zero-Dimensional (0D) models.....	15
2.2.2 One Dimensional (1D) models .....	16
2.2.3 Two Dimensional (2D) models .....	16
2.2.4 Three Dimensional (3D) models .....	17
2.2.5 Comparative of PEMFC models .....	18
2.2.6 PEMFC modelling and simulation tools .....	19
2.3 Applications of PEM fuel cells and balance of plant requirements .....	19
2.3.1 Automotive applications.....	19
2.3.2 Aerospace and aircraft systems .....	20
2.3.3 Heavy-duty and industrial applications .....	20
2.3.4 Heavy-duty and industrial applications .....	21
3 Theoretical background .....	22
3.1 Thermodynamic gas mixtures .....	22
3.2 Mass flow model .....	23
3.3 Cathode model.....	23
3.4 Anode flow model .....	24
3.5 Voltage model .....	24
3.5.1 Activation losses.....	25
3.5.2 Ohmic losses.....	25
3.5.3 Concentration losses .....	25
3.5.4 Actual cell voltage .....	26
3.6 Stack current .....	26
3.7 Stack Power and Efficiency.....	26
4 DISCUSSION.....	28
4.1 Model assumptions and clarifications .....	28
4.2 Simulation of Load Conditions for Model Validation.....	29
4.3 Cathode oxygen balance and partial pressure calculation .....	29
4.4 Anode Hydrogen Balance and Partial Pressure Calculation .....	30
4.5 Voltage model and stack potential calculation .....	30
4.6 Stack power .....	30
4.7 Stack efficiency .....	31
4.8 Comparison of PEMFC stack voltage models.....	31
CONCLUSION .....	33
REFERENCES .....	34
NOMENCLATURE .....	38

## Introduction

Over the past few decades, the world has witnessed the depletion of fossil fuel resources and the deterioration of our environment. The climate changes are imminent by unusual climate occurrences such as rains in the deserts, floodings above historical margins and dry periods on rainforests [1, 2]. Since the industrial era the human activity increased by 1°C global land surface air temperature and it still expected to increase to 1.5°C between 2030 and 2050 [3].

Transformations over different markets such as energy, transportation, manufacturing industry, and land use are demanded to achieve the goal in order to mitigate human adverse effects of climate change and promote sustainable development, as stated by [4]. This requires significant reductions in GHG emissions, aiming for net-zero carbon emissions in the EU as stated from the European Green Deal [5].

Hydrogen technologies play a significant role towards carbon neutrality, offering a promising pathway to reduce the environmental impacts of conventional energy sources. When produced using renewable energy sources, hydrogen generation becomes a carbon-neutral or even carbon negative alternative [6].

Fuel cell systems are a reliable solution towards decarbonization that from the electrochemical reaction of hydrogen and oxygen, able to generate electrical energy, heat and water as a product [7]. Different configurations exist according to operating temperature, efficiency, applications and costs, distinguished into 6 different groups and the polymer exchange membrane FC is ideal for vehicles, power plants, and portable power supplies with high economic, environmental, and technical benefits [8].

In power generation, Proton Exchange Membrane Fuel Cells (PEMFCs) are used in a multi-stack configuration (MFCs) to cater to high power requirements for large-scale application. A power plant obtaining hydrogen from Chlor-alkali industry was able to produce over 13.7 GWh of electricity within a two years span. Modelled, developed and tested from a 2MW stack [9].

A hybrid system with a PEM fuel cell battery system was developed in Korea to power a 20m long vessel for transporting tourists, capable of generating 56kW from fuel cell stack and 85kW combined power, being able to operate for 9 hours without refuelling. The system was demonstrated and it's being prepared for deployment [10].

A systematic review around emissions, lifecycle costs and performance of commercial hydrogen fuel cell electric vehicles (HFCEVs) outperformed conventional ICEVs in terms of fuel economy and well-to-wheel GHG emissions. HFCEVs showed significantly lower GHG emissions, with reductions ranging from 31% to 80% compared to conventional vehicles. However, the total cost of ownership for HFCEVs is still significantly higher due to the high costs associated with hydrogen production, storage, and fuel cell technology [11].

In the aviation industry, the EU is funding the Newborn Project to bring aviation graded fuel cells to market. Goals include achieving a 50% propulsion system efficiency by 2026, demonstrating scalable fuel cell power technology with a power density over 1.2 kW/kg [12]. The project also focuses on high power density energy conversion, propulsion systems, and next generation heat exchangers, developing a technology demonstrator for Clean Aviation program [13].

This thesis develops a zero-dimensional PEMFC model that integrates explicit thermal treatment at 353 K, physically grounded Tafel- and Ohm-law overpotential formulations, a lumped membrane-hydration submodel linking water content to proton conductivity, and calibrated mass-transport dynamics. A single-parameter least-squares tuning aligns the model's voltage-current curve with a benchmark, yielding a Mean Absolute Error of 0.6767 V and a Mean Relative Error of 1.45 %. Stack power, efficiency, and 3D voltage-current-power surfaces confirm numerical stability and predictive accuracy. The results are satisfactory for control-oriented and system-level

studies, and future work will validate these predictions against detailed experimental polarization, transient, thermal-management, and hydration data to support real-world PEMFC integration.

## 1 The energy sector, environmental challenges and the role of fuel cells

The global energy sector stands at the intersection of urgent environmental pressures and unprecedented opportunity for technological development. As the impacts of climate change become increasingly evident and global energy needs continue to grow, there is a growing effort on transitioning toward lower carbon emitting energy systems that can support environmental sustainability and economic development. This section outlines the driving forces behind the global energy transition, the limitations of current energy infrastructure, and the rising demand for clean and flexible energy carriers. Within this context, hydrogen and fuel cell technologies are gaining recognition as key enablers of deep decarbonization, particularly in sectors like heavy transport and distributed power generation.

### 1.1 Climate and energy system demands

The 21st century faces a defining challenge in the form of climate change, driven primarily by the accumulation of greenhouse gases (GHGs) in the atmosphere due to anthropogenic activities. According to the Intergovernmental Panel on Climate Change (IPCC), limiting global warming to 1.5°C above pre-industrial levels requires reducing global net anthropogenic CO<sub>2</sub> emissions by approximately 45% from 2010 levels by 2030 and reaching net-zero by around 2050 [56].

The energy sector remains the largest contributor to global GHG emissions, accounting for approximately 73% of total emissions when including electricity, heat, transport, and industry [57]. Fossil fuel combustion for electricity generation, industrial heat, and transport continues to dominate the global energy mix, despite recent growth in renewable sources. The dependence on fossil fuels also presents geopolitical vulnerabilities and economic volatility due to price fluctuations and supply constraints.

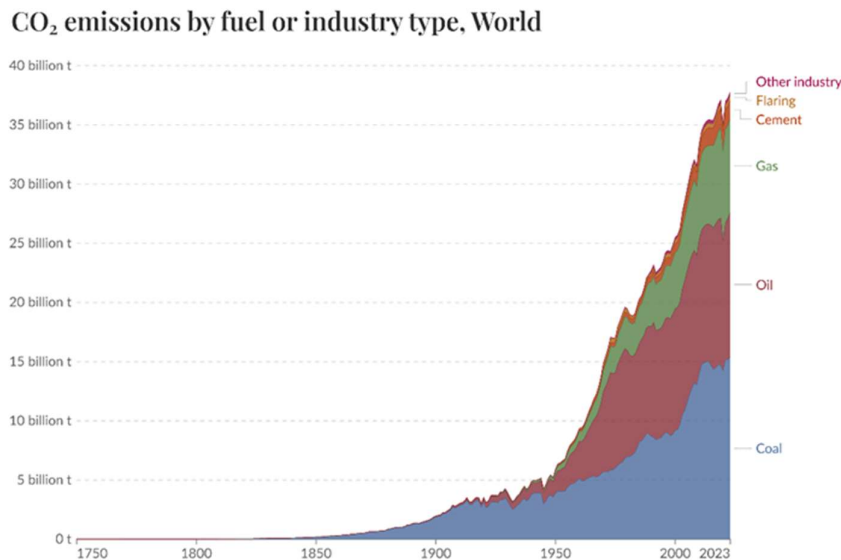


Fig. 1.1 – Share of CO<sub>2</sub> emissions by fuel industry worldwide

In parallel, growing urbanization, electrification of sectors, and the proliferation of digital infrastructure are driving up global energy demand. The International Energy Agency (IEA) projects that global electricity demand will grow by more than 60% by 2040, with a significant portion coming from developing economies [58]. Meeting this demand sustainably requires not

only the decarbonization of electricity production but also deep integration of renewable energy, energy storage, and flexible grid infrastructure.

The challenges are particularly acute in the transportation sector, which accounts for nearly 25% of global CO<sub>2</sub> emissions and is heavily dependent on oil-based fuels [59]. While battery electric vehicles (BEVs) are gaining traction, limitations in range, charging time, and energy density barriers in heavy duty and long-range applications. This creates a critical need for complementary technologies such as hydrogen fuel cells that can support deep decarbonization, especially where direct electrification is impractical.

In response, international frameworks like the Paris Agreement and regional initiatives such as the European Green Deal have set ambitious climate neutrality goals. The European Union aims to become the first climate neutral continent by 2050, targeting a 55% reduction in GHG emissions by 2030 compared to 1990 levels [60]. Achieving such goals requires a broad portfolio of technologies, including renewables, carbon capture, energy efficiency, and clean hydrogen pathways among which fuel cell technologies play a crucial role.

## 1.2 Hydrogen and fuel cells in energy transition

To achieve decarbonization goals across sectors such as industry, power, and transport, a diverse portfolio of clean energy solutions is required. Among these, hydrogen is emerging as a cornerstone of the global energy transition due to its versatility, high energy content, and ability to serve as both an energy carrier and a feedstock. When produced via electrolysis using renewable electricity, known as green hydrogen, becomes a zero emission fuel with potential to decarbonize sectors that are difficult to directly electrify [61].

Hydrogen can be stored over long periods, transported over long distances, and used in multiple end use applications including fuel cell systems, industrial processes, heating, and synthetic fuel production. Its role as a seasonal energy buffer also complements the variability of renewable power sources like wind and solar [62].

Fuel cells, particularly Proton Exchange Membrane Fuel Cells (PEMFCs), play a vital role in converting hydrogen into useful energy. Unlike combustion based power generation, fuel cells produce electricity through electrochemical reactions, emitting only water and heat as byproducts. This makes them inherently cleaner, quieter, and more efficient. PEMFCs operate at relatively low temperatures (60–80°C), feature quick start-up times, and can be scaled from watts to megawatts, making them especially attractive for mobile and distributed power applications [63].

The contribution for energy transition from the fuel cells has a wide possible applications like in Fuel cell electric vehicles (FCEVs), offers fast refueling and long range performance, with notable improvements in heavy duty applications such as buses, trucks, trains and ships [61]. Stationary fuel cells in the other hand, can provide backup power and combined heat and power (CHP) for buildings and industrial sites, where it can be integrated in hydrogen production with its power generation, forming a energy system [63,64].

The strategic relevance of hydrogen and fuel cells is reflected in numerous policy and funding initiatives. The European Union's Hydrogen Strategy (2020) aims to install at least 40 GW of renewable hydrogen electrolyzers by 2030 and produce up to 10 million tonnes of green hydrogen [64]. Countries like Japan, South Korea, Germany, and the United States have also launched national hydrogen roadmaps and committed significant investments to accelerate hydrogen deployment and fuel cell adoption [65].

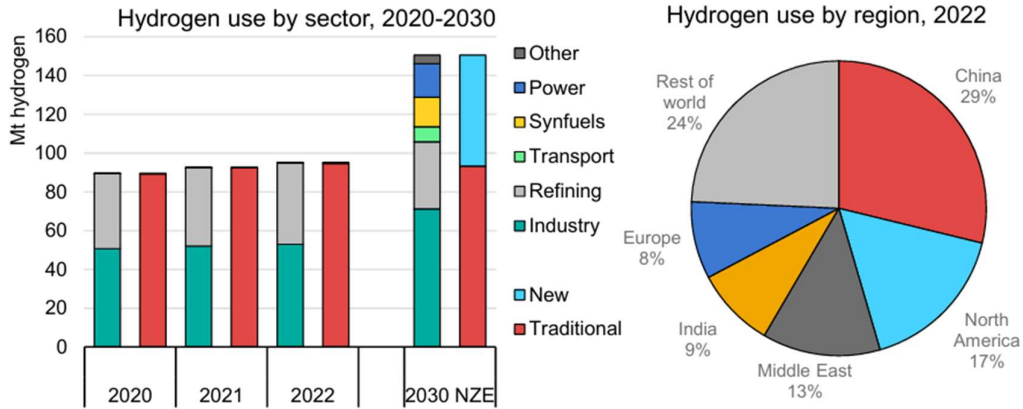


Fig. 1.2 – Projected hydrogen use by sector and region, 2020-2030 [10#]

Nevertheless, several challenges remain. These include reducing the cost of hydrogen production and distribution, scaling up infrastructure (such as refueling stations), improving fuel cell durability, and developing standards for safety and interoperability. Continued advances in materials science, manufacturing, and systems engineering are essential to overcome these barriers and unlock the full potential of hydrogen technologies in the energy transition [65].

As demonstrated, hydrogen and fuel cell technologies offer a compelling pathway toward a cleaner, more resilient energy system, with wide ranging applications in mobility, power, and industrial sectors. However, to fully understand the role and potential of fuel cells in practice, it is necessary to explore their internal operating principles, key components, and performance characteristics. The following section provides a technical foundation on fuel cell fundamentals, focusing particularly on Proton Exchange Membrane Fuel Cells (PEMFCs), which are widely regarded as one of the most promising fuel cell types for commercial deployment.

## 2 Fuel cell principles

A fuel cell is a device that transforms the energy of chemical reaction into electricity, producing water and heat as byproducts. The structure of a simplified fuel cell is shown in Fig. 1 [14]. The fuel cell comprises an electrolyte layer positioned between two electrodes. Hydrogen fuel is supplied to the anode electrode, while the oxidant (or oxygen from air) is supplied to the cathode electrode.

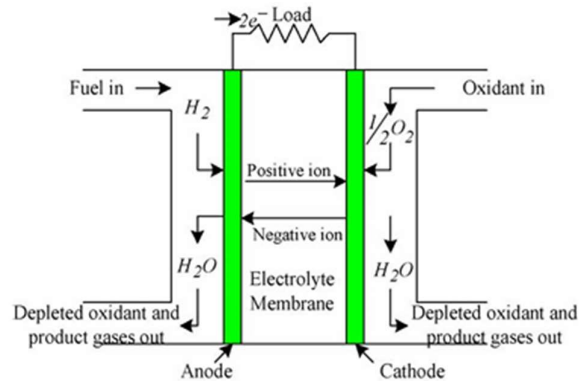
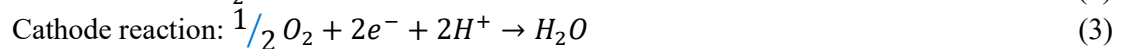


Fig. 2.1 – General fuel cell

The intermediate electrolyte membrane allows only the positive ions to flow from the anode to the cathode side, acting as an insulator for electrons. These electrons seek to recombine on the other side of the membrane for the system to stabilize, which causes the free electrons to move to the cathode side through an external electrical circuit. At the cathode, the recombination of the positive and negative ions with the oxidant occurs, resulting in depleted oxidant (or pure water) [15]. The chemical reactions at the anode and cathode, along with the overall reactions, are detailed below:



There are different types of fuel cells, distinguished mainly by the type of electrolyte used. The differences in cell characteristics, such as cell material, operating temperature, and fuel diversity, make each type of fuel cell suitable for different applications.

### 2.1 Polymer Electrolyte Membrane Fuel Cells

The Polymer Electrolyte Membrane Fuel Cells (PEMFC) are particularly suited for automotive applications due to their high-power density, solid electrolyte, and long operational life, combined with low corrosion rates. Operating at temperatures between 50 and 100°C, PEMFCs provide safer operation and eliminate the necessity for thermal insulation [16].

The polymer electrolyte membrane is a crucial component, acting as a conductor of hydrogen ions (protons) while being an electronic insulator. This membrane generally consists of a fluorocarbon backbone attached with sulfonic acid groups (SO<sub>3</sub>H<sup>+</sup>). When hydrated, these acid groups allow the transition of hydrogen ions (H<sup>+</sup>), which are essential for the electrochemical reactions within the cell [17].

The membrane is positioned between the anode and the cathode. These electrodes are made from conductive materials such as porous graphite. To enhance the rate of the electrochemical reactions, a small amount of platinum is applied to the surface of both electrodes. This platinum acts as a catalyst, increasing the efficiency of the hydrogen oxidation at the anode and the oxygen reduction at the cathode [18]. The combination of the anode, electrolyte, and cathode forms a single membrane electrode assembly (MEA), which is typically less than a millimetre thick [19]. See figure 2:

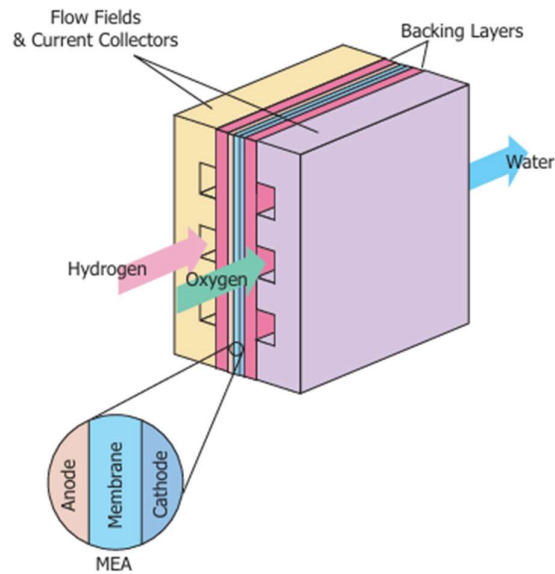


Fig. 2.2 – PEM Fuel cell

The properties of these membranes can vary significantly depending on the manufacturer and the specific type of membrane used, with thicknesses typically ranging from 50 to 175 microns [20].

## 2.2 Review of PEMFC modelling

Proton Exchange Membrane Fuel Cells (PEMFCs) can be modeled at different complexity levels, regarding the selection of the appropriate modelling approach towards the objective of the model. Depends not only on the required physical fidelity but also on practical factors such as the simulation objectives, available data, user expertise, and resource constraints (e.g., time, budget, and computational capacity).

The concept model selection should begin by defining the purpose of the simulation whether for educational purposes, detailed electrochemical analysis, component sizing, or vehicle-level integration. This definition informs the necessary model boundaries (cell, stack, or full system), time domain (steady-state vs. transient), and level of detail (empirical vs. physics-based).

A detailed 3D model might be necessary for analyzing current density non-uniformities, while a validated 0D model may be sufficient for fast evaluation of drive cycles or real-time control design. Additional important considerations include flexibility, availability of source code, and model validation, especially when integrating models into system-level tools or vehicle simulations. [21, 22]

### 2.2.1 Zero-Dimensional (0D) models

Zero-dimensional (0D) models represent the fuel cell as a lumped system, with no spatial resolution within cell components. The entire cell (or stack) is treated as a well-mixed control volume, assuming uniform conditions for temperature, species concentrations, and other state variables. In other words, a 0D model captures the overall input-output behavior and dynamic evolution of a fuel cell system without modeling gradients or distributions inside the cell. [23]

These models typically consist of algebraic equations for steady-state analyses and ordinary differential equations for dynamics of mass/energy storage and flows. The key phenomena such as the electrochemical reaction, membrane hydration, and gas dynamics are represented by simplified, averaged equations.

Zero-dimensional models often use empirical or semi-empirical relations for the model voltage losses due to activation, ohmic resistance and concentration gradients. All internal states (e.g. average membrane water content, average temperature) are assumed homogeneous. This approach is inherently *dynamic* (time-dependent) but zero-dimensional in space, i.e., it does not resolve variations along the cell's length, width, or thickness. [24,25]

Zero-dimensional models are widely used for *system-level simulation* and control design. Because they are computationally light, they can run in real-time or faster, making them suitable for integration into larger simulations of fuel cell systems (including balance-of-plant components like compressors, humidifiers, etc.) and for hardware-in-the-loop studies [26].

In automotive and power system contexts, 0D PEMFC models serve in evaluating drive cycles, optimizing control strategies (for startup, fuel/ air supply), and onboard diagnostics. A control-oriented PEMFC stack and system model for automotive applications capturing the dynamic air supply, hydrogen flow, and voltage response of a PEMFC system was developed and later even made open source. [27]

Industry toolsets like GT-Suite (Gamma Technologies) also provide 0D/1D fuel cell libraries, underscoring the industrial relevance of lumped modeling. *GT-SUITE* is an example of a commercial package that allows 0D and 1D fuel cell modeling and real-time simulation; it is considered a leading 0D–1D simulation tool and can even incorporate higher dimensional components if needed. Overall, 0D models are the workhorse for rapid simulations, control algorithm development, and preliminary design where detailed spatial information is not required [26, 28].

The main advantage of 0D models is their simplicity and computational efficiency, since they require relatively few inputs and parameters. Those parameters are usually global quantities, like total reactant flow rates and overall heat transfer coefficients that are simpler to parameterize and integrate with other system models [26].

Extensive scenario studies are conceivable due to the different time-step setups used for real time control implementation, and optimization loops that would be infeasible with higher dimensional models. Another benefit is that 0D models can directly include balance-of-plant dynamics. For instance, the lumped approach readily couples the entire fuel cell system behavior with auxiliary components (compressors, pumps, humidifiers) through ODEs, providing a holistic view of system performance and control [29].

The balance of plant dynamics with lumped approach are suitable for transient simulations (load changes, start/stop cycles) and for developing model based controllers or observers (state estimators) to infer internal states that sensors cannot measure. In summary, 0D models offer a fast and reasonably accurate way to predict overall PEMFC performance and efficiency under varying operating conditions, with less computational works [29,30].

However, the assumption of uniform conditions means that 0D models cannot capture spatial variations within the cell, such as local temperature gradients or reactant concentration disparities. This limitation can lead to inaccuracies in scenarios where such variations are significant.

Moreover, while they can incorporate many phenomena in aggregate, some detailed physics, like two-phase water dynamics or intricate catalyst layer kinetics, are challenging to model without adding complexity that contradicts the 0D philosophy [31].

Beyond automotive industry, 0D models have been utilized in stationary fuel cell system simulations, hybrid powertrain modeling, and the development of diagnostic techniques. Their tractability makes them a preferred choice for initial design stages, control system development, and subsystem integration testing [32].

### 2.2.2 One Dimensional (1D) models

Spatial resolution in a single direction is the defining feature of one-dimensional (1D) models for fuel cells. These models assume uniformity in the other two directions, allowing for the resolution of gradients across the membrane, catalyst layers, and gas diffusion layers (GDLs) [33]. Common simplifying assumptions include homogenous and isotropic material properties, negligible gradients in unmodeled directions, and the dominance of Fick diffusion over convective transport [34].

Such models are frequently employed to analyse phenomena within the membrane and electrodes, particularly hydration profiles and voltage distribution [35]. They are also applied to along-channel analyses, capturing effects like fuel depletion and current density gradients from inlet to outlet [34]. At the stack level, 1D modelling is used to examine axial variations in temperature and water content [36]. More recently, hybrid 1D+1D frameworks have been introduced to approximate two-dimensional effects with improved computational efficiency [37].

By resolving species, temperature, and hydration gradients, 1D simulations offer improved physical fidelity compared to zero-dimensional (0D) models, particularly for membrane and gas diffusion layer studies [35, 38]. The structure is compatible with analytical or semi-analytical formulations, supporting experimental calibration and model-based control development [32].

However, 1D approaches have limitations. They cannot resolve lateral (in-plane) variations such as localized flooding or oxygen starvation in complex geometries [36]. Accuracy also depends heavily on reliable material property data and proper calibration, which can be sensitive to input uncertainties [31]. Dynamic and two-phase implementations add realism but also increase computational cost relative to 0D approximations, making them most suitable where dominant gradients align with the modelled direction [38].

Several practical implementations highlight the utility of this modelling approach. A membrane hydration study quantified how water transport from anode to cathode influences conductivity [35], while another model accurately predicted polarization behaviour by incorporating catalyst layers [38]. A dynamic 1D stack model has been developed for real-time simulation [26], and a hybrid 2D/1D framework has been used for component-level and system-level co-simulation. These techniques have found their way into commercial platforms such as gPROMS and MATLAB/Simulink [37].

### 2.2.3 Two Dimensional (2D) models

Two-dimensional models resolve spatial variations in two directions typically the through plane and along channel axes, offering a more detailed representation of internal PEMFC behavior than 0D and 1D approaches. These models solve coupled partial differential equations (PDEs) for mass, momentum, heat, and charge transport, along with electrochemical reactions throughout the membrane-electrode assembly and flow fields [39]. The inclusion of spatial gradients in species concentration, temperature, and current density enables more realistic simulation of operational dynamics.

These models are widely used to study how design parameters and operating conditions affect fuel cell performance. Applications include investigations of patterned wettability in gas diffusion layers (GDLs) for improved oxygen diffusion and water removal, analyses of magnetic field

distribution within stacks for diagnostic purposes, and evaluations of heat and water management strategies [40, 41, 42].

Two-dimensional modeling strikes a balance between physical detail and computational efficiency. By capturing spatial distributions of key variables such as current density, water content, and temperature, it enables effective diagnosis of performance limiting factors and supports geometric optimization [41, 42].

Despite their advantages, 2D models simplify the third spatial dimension, which can lead to overlooked phenomena such as lateral nonuniformities induced by serpentine flow fields. They also require more computational resources and a greater quantity of accurate material and operating parameters [40].

Several studies have demonstrated the value of 2D modeling. One model successfully reproduced oxygen and water vapor profiles under variable conditions [39]. Another showed that modifying GDL wettability patterns could significantly improve liquid water management [22]. Magnetic field effects on stack diagnostics have been analyzed using layered 2D simulations [20], while the impact of hydrogen starvation on anode polarization was also explored using this modeling framework [21].

#### **2.2.4 Three Dimensional (3D) models**

Three-dimensional (3D) models provide a full spatial resolution of a PEMFC across the through-plane, along-channel, and cross-channel directions. These models solve coupled partial differential equations describing multiphase flow, multi-component species diffusion, heat and charge transport, and electrochemical reactions throughout all major components of the cell. They are particularly valuable for analyzing water management strategies, thermal effects, and reactant distribution within the cell [43].

An unsteady, non-isothermal, two-phase 3D-CFD model of a large active area PEMFC, which utilized experimental data for parameterization and validation was developed by [43]. The work emphasized the simulation of internal water formation, transport processes during load changes, and visualization of the self-humidification strategy of the cell gases.

The model incorporated a homogenized channel meshing strategy to reduce computational cost while maintaining fidelity required to capture local variations in current density, membrane hydration, and liquid water saturation under automotive operating conditions. The model parametrization and simulated transient behaviors, provided insights into water formation and transport processes during load changes[43].

A 3D multiphase flow CFD model optimized parallel flow field in PEMFC, enhancing water removal and reducing transport resistance [44]. Additionally, 3D models have been utilized to study the impact of catalyst layer structures on fuel cell performance. A 3D model incorporating an agglomerate sub-model of the cathode catalyst layer to accurately capture the effects of catalyst loading, provided understanding of the electrochemical processes within the cell [45]

Compared to lower dimensional models, 3D models provide accurate insights into spatial distributions of current density, temperature, and water content [46]. They enable detection of localized phenomena such as hot spots, flooding, and starvation. The models are useful for testing novel geometries and material configurations *in silico* before physical prototyping [44].

Despite their advantages, 3D models are computationally expensive and require high-quality, detailed input data. Accurate boundary conditions, geometry, and material properties must be known or estimated, which can be a significant challenge. Their validation also often depends on extensive experimental datasets, which may not always be available [43]. These constraints have motivated hybrid approaches, like combining 3D physics with reduced-order surrogates for real-time simulation.

Using a refined 3D mesh, flow fields that improve water removal and mass transport in PEMFC stacks, leading to performance and durability improvements were developed [47]. By

integrating degradation models with 3D simulations, researchers can predict the effects of material aging and operational stresses on fuel cell longevity [48].

Combining 3D modeling with machine learning techniques, such as deep learned super resolution and multi label segmentation, allows for high-fidelity simulations that can predict complex behaviors within the fuel cell, leading to more accurate and efficient designs [49].

### 2.2.5 Comparative of PEMFC models

This section summarizes the comparative characteristics of zero-dimensional (0D), one-dimensional (1D), two-dimensional (2D), and three-dimensional (3D) modeling approaches for PEMFC. Each approach offers distinct advantages and limitations in terms of fidelity, computational requirements, and suitability for various engineering tasks. The comparison is synthesized from reviewed sources [23, 26, 31, 32, 43, 45].

Tab. 2.1 Comparison of PEMFC modelling.

	0D Models	1D Models	2D Models	3D Models
<b>Dimensionality</b>	Lumped (no spatial resolution)	Through-plane or along-channel	Through-plane + in-plane	Full 3D spatial resolution
<b>Governing Equations</b>	Algebraic + ODEs	ODEs + simplified PDEs	Coupled 2D PDEs	Coupled 3D PDEs (multiphysics)
<b>Spatial Resolution</b>	None	Single axis (x or y)	Two axes (x and y)	Three axes (x, y, z)
<b>Computational Cost</b>	Very Low (real-time)	Low to Moderate	Moderate	High
<b>Simulation Time</b>	Milliseconds to seconds	Seconds	Minutes	Hours (or more)
<b>Data Requirements</b>	Low (average/global parameters)	Medium (membrane/GDL properties)	High (flow field, thermal)	Very high (materials, geometry, BCs)
<b>Applications</b>	Control design, HIL, energy management	Membrane/GDL studies, real-time simulation	Heat/water analysis, flow-field testing	High-fidelity design, diagnostics
<b>Phenomena Captured</b>	Global trends	Hydration, diffusion in 1D	In-plane gradients, transport paths	Hotspots, flooding, gas/multiphase flow
<b>Implementation Complexity</b>	Simple (few equations)	Moderate	Moderate to high	Complex (mesh, solvers, data handling)
<b>Real-Time Capability</b>	Excellent	Good	Poor	Not feasible
<b>Example References</b>	[23], [26], [29]	[33], [34], [35]	[39], [40], [42]	[43], [44], [45], [49]

As shown in Table 2.1, the choice of model dimensionality depends on the simulation goals and constraints. Zero-dimensional models are highly suitable for real-time and control applications, while 3D models offer unmatched physical detail for design and diagnostics. Intermediate-dimensional models (1D and 2D) provide useful trade-offs, balancing computational efficiency and spatial fidelity.

### 2.2.6 PEMFC modelling and simulation tools

MATLAB/Simulink is focused Control systems, system-level simulation contemplating model-based design with graphical environment, allows integration with balance-of-plant systems with real time simulation and code generation. Not suited for detailed 3D simulations but widely used in control development and embedded systems [50].

GT-SUITE is a 0D/1D/3D simulation tool for conducting simulations of control systems and solving real-time simulations, aiming System-level design and vehicle simulation in different operating scenarios. The key advantages rely on detailed fuel cell and balance of plant modeling capable of Integrated thermal, fluid, and electrical domains. It is limited to automotive applications, but powerful for engine systems and fuel cell vehicle design [51].

COMSOL Multiphysics targets Multiphysics FEM simulation, enabling Coupled physics modeling (electrochemistry, heat, mass) under customizable multiphysics environments. Computational intensity and additional cost with specific software modules are the main constraints, however it is suitable for detailed stack and component simulations [52].

ANSYS Fluent aims CFD and multiphase analysis with advanced flow and thermal simulations and detailed transport and reaction modeling. The main constraints are high computational and setup demands on fine meshing and boundary conditions. Applied for flow field design and thermal management [53].

Siemens Simcenter Amesim targets multidomain vehicle system simulation with prebuilt libraries for fuel cell systems, system-level energy and control evaluation. Constrained by High complexity for basic uses requiring understanding of the Simcenter Amesim environment. Applied in FCEV simulation and range estimation [54].

## 2.3 Applications of PEM fuel cells and balance of plant requirements

Proton Exchange Membrane Fuel Cells (PEMFCs) are gaining broad adoption due to their modular architecture, rapid load-following capability, and efficient operation at relatively low temperatures. Successful implementation depends not only on the fuel cell stack but also on a carefully designed balance of plant (BoP), which typically includes systems for air and hydrogen supply, thermal and water management, humidification, and power conditioning.

### 2.3.1 Automotive applications

Proton Exchange Membrane Fuel Cells (PEMFCs) are gaining broad adoption in the automotive sector due to their high energy conversion efficiency, zero-emission operation, and compatibility with renewable hydrogen sources [1], [6], [12]. Their suitability for mobility applications stems from their modular architecture, rapid load-following capability, and efficient operation at relatively low temperatures [10], [27]. However, successful vehicle integration depends not only on the fuel cell stack itself but also on a carefully designed balance of plant (BoP), which includes systems for air and hydrogen supply, thermal and water management, humidification, and power electronics [11], [13].

PEMFCs are central to fuel cell electric vehicles (FCEVs), offering advantages such as quick refueling, high gravimetric energy density, and suitability for long-range and commercial transport missions. The BoP in automotive systems generally integrates components such as:

- Air compressors with associated humidifiers
- Hydrogen supply and recirculation loops
- Thermal management loops with radiators, pumps, and thermostatic bypasses
- Water recovery systems (condensers, reservoirs)
- DC-DC converters and hybridization interfaces

Pukrushpan et al. demonstrated that PEMFCs can achieve system efficiencies between 50% and 60%, particularly when integrated with hybrid drivetrains and regenerative braking [27]. These configurations benefit from compact, responsive BoP architectures that can adapt to highly transient power demands during drive cycles..

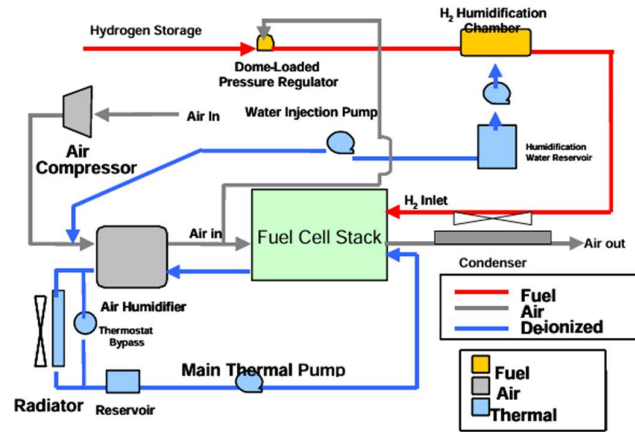


Fig. 2.5 – Fuel cell system schematics

A detailed example of such a configuration is illustrated in the fuel cell system schematic from Gurski's thesis [Gurski, 2002], based on the Virginia Tech *Magellan* hybrid fuel cell SUV. This diagram (Figure X) clearly shows the structural integration of thermal, air, and hydrogen subsystems. Notably, the design includes a water injection pump, dome-loaded pressure regulators, and a humidifier loop using coolant waste heat—elements that enable effective membrane hydration and cold-start performance. Gurski's analysis also quantified how low stack temperatures significantly reduce system power output and efficiency, emphasizing the importance of well-designed thermal subsystems and hybrid buffering under transient or sub-optimal conditions.

### 2.3.2 Aerospace and aircraft systems

In aerospace, PEMFCs are being actively explored for auxiliary power units (APUs), unmanned aerial vehicles (UAVs), and next generation hybrid electric propulsion systems. Projects such as the EU Newborn initiative and H2FLY's HY4 program target scalable and certifiable aviation fuel cell systems. The HY4 aircraft became the first four-seat hydrogen-electric aircraft to complete a piloted flight, demonstrating the viability of PEMFCs at altitude with a specific power target above 1.2 kW/kg and system efficiency beyond 50% [12].

Achieving these performance levels requires highly integrated BoP systems, including lightweight compressors, altitude-adapted heat exchangers, and fault-tolerant hydrogen and oxygen delivery subsystems. The powertrains must also maintain thermal and electrical stability under rapid altitude and load changes typical in aerospace operation.

### 2.3.3 Heavy-duty and industrial applications

For heavy-duty vehicles like freight trucks and trains, PEMFCs offer high torque, long range, and rapid refueling. Choi et al. reported successful validation of over 100 kW class PEMFC systems with under-15-minute hydrogen refueling times [10]. In such systems, the BoP must manage multi-stage air compression, durable thermal circuits, and high-capacity hydrogen logistics. European field trials have reinforced their suitability in harsh duty cycles [11].

#### **2.3.4 Heavy-duty and industrial applications**

In stationary applications, PEMFCs support backup power, distributed energy generation, and combined heat and power (CHP) units. According to Zheng et al., these systems can be economically optimized through integration with onsite hydrogen reforming and automated thermal recovery [6]. Further studies have shown their potential in renewable-powered microgrids, where fuel cells work alongside solar panels and electrolyzers to form sustainable, closed-loop energy networks [7][8].

### 3 Theoretical background

#### 3.1 Thermodynamic gas mixtures

The ideal gas law is a fundamental thermodynamic relationship used to link pressure, temperature, and volume to the amount of gas present in a system to its mass or molar amount. In PEMFC modelling, it serves as a crucial tool for estimating the partial pressures of gaseous species (hydrogen, oxygen, water vapor) within the anode and cathode compartments under the assumption that these gases behave ideally [3\*,6\*,17].

The ideal gas law is expressed as:

$$PV = mRT \quad (4)$$

Where P is the gas absolute pressure (Pa), V is the volume (m<sup>3</sup>), m is the mass of gas (kg), T is the absolute temperature (K). When evaluated in molar basis, the term *m* (mass of gas) becomes *n* (number of moles) and the universal gas constant should be given accordingly, in molar mass base and the unit is J/mol\*K or g/mol\*K.

In a PEMFC, partial pressures of individual species are critical because they directly influence the electrochemical performance via the Nernst equation [14], [17]. Assuming homogeneous mixing and ideal gas behavior, the partial pressure of a species is derived from its mass, for the cathode:

$$p_{O_2} = \frac{m_{O_2} R_{O_2} T_{fc}}{V_{ca}} \quad (5)$$

And for hydrogen in the anode:

$$p_{H_2} = \frac{m_{H_2} R_{H_2} T_{fc}}{V_{an}} \quad (6)$$

Where *p*, *m*, and *R* yields partial pressure, mass and universal gas constant of oxygen and hydrogen respectively. *T<sub>fc</sub>* is the fuel cell stack temperature (K), *V<sub>ca</sub>* is the volume of the cathode and *V<sub>an</sub>* is the volume of the anode both in m<sup>3</sup>. These calculations are valid under the assumption of ideal gas behavior for all species, constant and uniform temperature across the entire stack, negligible heat transfer (adiabatic assumption) and homogeneous mixing within control volumes (0D) [23], [26], [32].

In addition to pressure and temperature, the water vapor content in the anode and cathode gases critically influences PEMFC operation. This can be quantified using the humidity ratio:

$$\omega = 0.622 \frac{P_v}{P - P_v} \quad (7)$$

Where *P<sub>v</sub>* is the partial pressure of water vapor and *P* is the total gas pressure. The Specific Humidity (*φ*) is the mass of water vapor per unit mass of the moist air (or gas mixture):

$$\varphi = \frac{m_v}{m_{dry} + m_v} = \frac{\omega}{(1 + \omega)} \quad (8)$$

Where *m<sub>v</sub>* is the mass of water vapor in the mixture and *m<sub>dry</sub>* denotes the mass of dry air. These humidity parameters are used for membrane hydration modeling, which affects proton conductivity and ohmic resistance [14], [26]. In terms of the water transport through the membrane the dependency of electro-osmotic drag and back diffusion on the humidity ratio and specific humidity enable supporting water management strategies in balance of plant components (e.g., humidifiers, heat exchangers) [24].

By integrating the ideal gas law with partial pressures and humidity metrics, PEMFC models can dynamically track gas compositions in the anode and cathode, predict partial pressures, which

influence Nernst voltage and reactant availability, estimate membrane water content and thermal behavior, inform control strategies for temperature, humidification, and reactant flows. These assumptions aligns with 0D modelling and are suitable for real time simulation and control design where spatial gradients are neglected [23], [26], [17].

### 3.2 Mass flow model

In PEMFCs modeling of mass balances for hydrogen, oxygen, and water vapor is critical to capture the dynamic behavior of species transport and reaction within the cell. The governing equations describe transient species accumulation based on mass flow in, out, and consumed within the fuel cell compartments [17, 55]. Mass balance equations are typically derived from the law of conservation of mass. For a control volume, the general form of the mass balance for a species is:

$$\frac{dm}{dt} = \frac{dm_{in}}{dt} - \frac{dm_{out}}{dt} \pm \frac{dm_{gen}}{dt} \quad (9)$$

This principle is applied in the current discrete time model for the cathode and anode compartments of the PEMFC.

### 3.3 Cathode model

The cathode side of the PEMFC involves mass balance modeling for the air stream entering and exiting the cathode compartment, which consists primarily of oxygen, nitrogen, and water vapor. The oxygen participates in the electrochemical reaction, the nitrogen serves as an inert carrier gas, and the water vapor is generated during the reaction or transported across the membrane.

The model accounts for the incoming and outgoing mass flows of each media as well as generation and transport processes, assuming a zero dimensional (0D) control volume where the compartment is treated a uniform system with no spatial variations. This approach captures the dynamic evolution of species concentrations and is particularly suitable for control oriented and system level simulations, consistent with modeling frameworks in the literature [23], [26].

The rate of change in the mass of cathode oxygen is given by the mass balance:

$$\frac{dm_{ca}}{dt} = \frac{dm_{O_2}}{dt} - \frac{dm_{N_2}}{dt} + \frac{dm_{w,ca}}{dt} \quad (10)$$

The rate of oxygen flow is given by:

$$\frac{dm_{O_2}}{dt} = W_{O_2,in} - W_{O_2,out} - W_{O_2,rct} \quad (11)$$

The rate of water vapor in the cathode is given by:

$$\frac{dm_w}{dt} = W_{gen} - W_{w,membr} - W_{w,out} \quad (12)$$

The rate of the purging nitrogen flow is governed by:

$$\frac{dN_{O_2}}{dt} = W_{N_2,in} - W_{N_2,out} \quad (13)$$

Hence the mass flow rate of air entering the cathode is:

$$W_{ca,in} = W_{O_2,in} + W_{N_2,in} \quad (14)$$

And the mass flor rate of air exiting the cathode:

$$W_{ca,out} = W_{O_2,out} + W_{w,out} \quad (15)$$

Where  $m_{ca}$  is the total mass flow rate across the cathode, respectively  $m_{O_2}$ ,  $m_{N_2}$  and  $m_w$  are the mass flow rates of oxygen, nitrogen and water vapor.  $W_{O_2,rct}$  is the amount of oxygen reacted,  $W_{w,membr}$  is the amount of water vapor across the electrolyte membrane and  $W_{gen}$  is the amount of water produced by the electrochemical reaction [17].

The electrochemistry principles are used in oxygen consumption and water production calculations in function of the stack current  $I_{st}$  according to Faraday law [17]. The reacted oxygen is given by:

$$W_{O_2,rct} = M_{O_2} \frac{n_{cells} I_{st}}{4F} \quad (16)$$

And the water produced by the electrochemical reaction:

$$W_{m,rct} = M_{H_2} \frac{n_{cells} I_{st}}{2F} \quad (17)$$

Where the molar masses are denoted by  $M_{O_2}$  for oxygen and  $M_{H_2}$  for hydrogen,  $n_{cells}$  is the number of cells in the stack and F is the Faraday number.

### 3.4 Anode flow model

The anode side contemplate the rate at which the mass of hydrogen inside the anode of the fuel cell changes:

$$\frac{dm_{an,in}}{dt} = W_{an,in} - W_{an,out} - W_{H_2,rct} \quad (18)$$

Where  $W_{an,in}$  is the mass flow rate of hydrogen entering the anode,  $W_{an,out}$  is the mass flow rate of hydrogen leaving the anode and  $W_{H_2,rct}$  is the mass flow rate of reacted hydrogen, that can be determined by:

$$W_{H_2,rct} = M_{H_2} \frac{n_{cells} I_{st}}{2F} \quad (19)$$

These equations assume dry hydrogen at the inlet and ignore membrane crossover or condensed water removal, focusing on gaseous species dynamics. This simplification is suitable for control oriented dynamic modeling where spatial resolution is not necessary. The model follows 0D assumptions, treating the fuel cell zones as homogeneously mixed volumes with no spatial gradients, aligning with system level dynamic modeling approaches described in [23, 26,35].

These formulations reflect simplified but physically grounded approximations suitable for system level simulation, control development, and performance prediction in PEMFCs [12, 17]).

### 3.5 Voltage model

The Nernst equation determines the theoretical no load voltage of a PEM fuel cell and serves as the baseline for calculating actual cell voltage. In practical operation, this ideal voltage is reduced by various loss mechanisms such as activation, ohmic, and concentration overpotentials which account for kinetic, resistive, and mass transport limitations [14], [26].

Regarding the equation dependency on the partial pressures of hydrogen and oxygen, it connects to the gas mass balances in the anode and cathode, associating electrochemical performance to flow and consumption dynamics [24], [32]. Using expansion of the standard reversible cell voltage equation and thermodynamic standard values for entropy change, the reversible cell voltage E is given by the equation:

$$E = 1.229 - 0.85 * 10^{-3}(T_{fc} - 298.15) + 4.3085 * 10^{-5}T_{fc} \left[ \ln(p_{H_2}) + \frac{1}{2}\ln(p_{O_2}) \right] \quad (20)$$

Where  $T_{fc}$  is the fuel cell temperature and  $p_{H_2}$  and  $p_{O_2}$  are partial pressures for hydrogen and oxygen respectively. Further clarifications on the steps to achieve the simplifications were developed in [17].

Temperature also influences the Nernst voltage. While increasing temperature enhances the voltage logarithmically, it also introduces a linear drop via entropy effects, reflecting both kinetic and thermodynamic trade-offs [26], [19]. For this reason, the Nernst equation plays a key role in system level modelling and control, supporting the estimate voltage limits, guide hybrid power management, and support feedforward control strategies in real time applications [17], [32], [29].

The Nernst equation assumes equilibrium conditions and ideal gas behavior. Deviations under high current densities (flooding, drying, gas starvation) may necessitate empirical corrections or dynamic adaptation [31], [33]. Effects like crossover, membrane dehydration, and localized hot spots are not reflected in the Nernst equation but influence observed voltage significantly [20].

Despite these limitations, the Nernst equation remains the backbone of theoretical PEMFC voltage formulation and is embedded in virtually all model types, from 0D lumped to high fidelity 3D-CFD frameworks [23], [32], [26].

In real world PEM fuel cell operation, the actual cell voltage is lower than the ideal voltage predicted by the Nernst equation due to various irreversible losses. These losses, also known as overpotentials, fall into three main categories: activation loss, ohmic loss, and concentration loss. Each loss mechanism reflects a different physical limitation in the cell and must be modeled to accurately predict voltage and efficiency under load.

### 3.5.1 Activation losses

Activation losses, also known as kinetic overpotentials, arise from the energy barrier associated with initiating the electrochemical reactions at the electrodes. This is especially prominent at the cathode, where the oxygen reduction reaction is inactive. The activation overpotential  $v_{act}$  is modeled by the Tafel equation:

$$v_{act} = \frac{RT_{fc}}{\alpha F} \ln \left( \frac{I}{I_0 A_{cell}} \right) \quad (21)$$

Where  $R$  is the universal gas constant,  $T_{fc}$  is the fuel cell temperature,  $\alpha$  is the charge transfer coefficient,  $F$  is the Faraday number,  $I$  is the cell current [A],  $I_0$  is the exchange current density [A/cm<sup>2</sup>],  $A_{cell}$  is the electrode area [cm<sup>2</sup>]. Activation losses dominate at low current densities and are strongly affected by catalyst properties, temperature, and membrane hydration [14], [26].

### 3.5.2 Ohmic losses

Ohmic losses are caused by the resistance to proton flow through the membrane and electron flow through external circuits [26]. These are modeled by a simple Ohm's law expression:

$$v_{ohmic} = I_{st} R_{mem} \quad (22)$$

Where  $I_{st}$  is the stack current,  $R_{mem}$  is the total ohmic resistance [ $\Omega$ ] calculated from [17]. This loss increases linearly with current and is influenced by membrane thickness, water content, and contact resistance [31].

### 3.5.3 Concentration losses

Concentration losses can also called mass transport losses, they occur when reactant gases are consumed faster than they can be replenished at the reaction sites, leading to concentration gradients. They become significant at high current densities when diffusion limits are reached. The empirical form used is:

$$v_{conc} = -B \ln \left( 1 - \left( \frac{I_{st}}{I_{max}A_{cell}} \right) \right) \quad (23)$$

Where B is an empirical constant [V],  $I_{max}$  is the limiting current density [A/cm<sup>2</sup>] and  $A_{cell}$  is the electrode area [cm<sup>2</sup>]. These losses reflect limitations in gas diffusion through the porous electrode layers and are influenced by pressure, humidity, and flow field design [32], [24].

### 3.5.4 Actual cell voltage

The actual cell voltage is computed as:

$$V_{cell} = E - v_{act} - v_{ohmic} - v_{conc} \quad (24)$$

This formulation enables dynamic voltage prediction as operating conditions vary. These three loss terms are fundamental to both control oriented and detailed PEMFC models and are supported by extensive experimental and simulation studies [14], [26], [24], [32].

### 3.6 Stack current

Stack current determines the power output when multiplied by cell voltage. Accurate current prediction is therefore essential for modeling fuel cell performance, especially under transient load conditions [24], [32]. Stack current is calculated by rearranging the hydrogen consumption equation:

$$I_{st} = W_{H_2, rct} \left( \frac{2F}{M_{H_2} n_{cells}} \right) \quad (25)$$

This expression assumes each mole of hydrogen contributes two moles of electrons (2 Faradays), and that the reaction proceeds with 100% efficiency (i.e., all reacted hydrogen contributes to current generation). This formulation allows for direct coupling between hydrogen fuel supply, chemical reaction rate, and electrical output [17], [14], [26]. Furthermore, the current density can be computed by normalizing the stack current per active cell area [17]:

$$i_{stack} = \frac{I_{stack}}{A_{cell}} \quad (26)$$

In system level models, current serves as a primary control variable. It influences voltage losses, thermal generation, and water transport. It is used in control oriented models for designing feedback loops and power management strategies [29], [17]. Through Faraday's law, current enables back calculation of hydrogen consumption, a key metric for fuel economy and range prediction in mobile applications [26], [15].

Experimental measurements of current provide one of the most accessible means of validating fuel cell models. Discrepancies in simulated current often signal issues in the estimation of mass balances, pressure dynamics, or electrochemical kinetics [31], [32].

The stack current expression above is ideal for lumped parameter (0D) or control oriented models due to its simplicity and strong physical basis. It integrates seamlessly into multi domain simulations involving balance of plant components like humidifiers, compressors, and DC/DC converters.

### 3.7 Stack Power and Efficiency

The electrical power output of the fuel cell stack is determined by the product of the total stack voltage and current:

$$P_{stack} = V_{stack} I_{stack} \quad (27)$$

Where  $V_{stack}$  is the stack voltage per number of cells, and  $I_{stack}$  the total current drawn. This relationship forms the basis for power tracking and energy management in PEMFC system simulations [17].

The voltage efficiency of a PEM fuel cell is defined as the ratio of actual cell voltage to the open-circuit voltage predicted by the Nernst equation:

$$\eta_{voltage} = \frac{V_{cell}}{E} \quad (28)$$

This efficiency metric captures the cumulative impact of activation, ohmic, and concentration losses on fuel cell performance. It provides a useful scalar for comparing simulated and experimental system behavior, and is especially relevant in 0D models where thermal and fuel utilization efficiencies are not explicitly computed [23, 45].

Although full system efficiency can be defined in terms of enthalpy of hydrogen fuel, such formulations can be an alternative for more high-fidelity thermodynamic models. In control-oriented applications, voltage efficiency offers a direct and tractable measure of stack-level performance [17, 23].

## 4 DISCUSSION

The mathematical model developed in this master's thesis builds upon the zero-dimensional PEM fuel cell modeling framework presented by [55], which provides a simplified yet effective representation of fuel cell dynamics suitable for control-oriented and system-level simulations. To ensure alignment with validated physical behavior and to enhance the predictive capability of the model, key parameters and structural assumptions were initially adopted and subsequently calibrated against the published formulation in [55].

The validation data from [55], assumes a spatially uniform temperature throughout the fuel cell stack, they do not assign a specific numeric value in their model equations. Instead, temperature is treated symbolically and is referenced only in relation to its role in electrochemical equations such as the Nernst potential and activation overpotential [55]. In contrast, this thesis model incorporates the temperature explicitly across all domains, including gaseous phase mass balances, partial pressure calculations via the ideal gas law, and voltage loss mechanisms [55]. This approach ensures consistent thermodynamic conditions and enables more accurate simulation under defined thermal boundaries in their model.

The value of 353 K was selected based on the reference PEMFC operating temperature provided by [17], where 80 °C is used as the nominal stack temperature for modelling and control design purposes. This operating point is consistent with practical automotive and stationary PEM fuel cell systems, where thermal management is designed to maintain high membrane conductivity and stable electrochemical performance. The use of this temperature allows the model to reflect realistic thermal behaviour and facilitates comparison with other literature based implementations.

Additionally, the model presented here incorporates the activation, ohmic, and concentration voltage loss equations directly from [17] zero-dimension model, which offers widely validated formulations suitable for control oriented applications. This choice enables a direct comparison of voltage loss modeling strategies between the more empirically tuned formulation by [55] and the physically grounded loss mechanisms in Pukrushpan's approach. Notably, Saleh et al. derive activation losses from empirical coefficients fitted to experimental data, while Pukrushpan's model bases the loss mechanisms on the Tafel equation, Ohm's law, and empirical mass transport limitations providing clearer parametric sensitivity and generalizability.

Furthermore, the mass flow dynamics and electrochemical formulations in this thesis were refined, particularly in how hydrogen and oxygen consumption are linked to stack current via Faraday's law. However, to improve numerical stability and model fidelity, specific parameter values such as membrane resistance, exchange current density, and flow rates were adjusted through calibration against the experimental operating range described in their study [55].

### 4.1 Model assumptions and clarifications

Model simplifications enable computational efficiency and structural clarity, while retaining the physical fidelity required for system-level and control-oriented applications:

**Zero-dimensional:** Each compartment is modeled as a spatially uniform control volume. This lumped-parameter structure is widely accepted in control-oriented PEMFC models and validated for system-level simulation tasks [17, 23, 26].

**Ideal gas:** Hydrogen, oxygen, and water vapor are modeled as ideal gases. This holds true under typical PEMFC conditions, where deviations from ideality are minimal [45].

**Constant stack temperature:** A uniform stack temperature of 353 K is used throughout all computations.

Steady state and reactant flow rates: Reactant and product mass flow rates are assumed constant within each simulation step. This aligns with steady-state operating conditions in laboratory tests and simplifies dynamic mass balances [55]

Lumped water behavior: Membrane hydration and water transport are not modeled explicitly. Instead, water effects are reflected via calibrated ohmic resistance. This simplification is common in low-order models for control and estimation purposes [23].

Use of Faraday's law: Reactant consumption and water generation are directly tied to stack current through Faraday's law. This provides a robust and physically grounded link between electrochemical reactions and mass flows [17].

Voltage Loss Models Based on Tafel and Empirical Expressions: Activation, ohmic, and concentration losses are modeled using standard expressions from PEMFC literature. These formulations balance accuracy with numerical efficiency and are widely validated [17, 45].

Non-Negativity of Mass States: All gas species masses are bounded below by zero to ensure physical consistency and prevent numerical instability during dynamic simulation [17].

Simplified nitrogen and water treatment: Nitrogen is treated as inert, and water transport across the membrane is not explicitly resolved. These simplifications reduce model complexity while preserving key electrochemical behaviors for voltage prediction and system-level analysis [23].

## 4.2 Simulation of Load Conditions for Model Validation

In alignment with the validation protocol in [55], the simulated current profile is ramped from 1 A to 17 A, matching the operational envelope of the Horizon H-1000 PEMFC stack. This mirrors the experimental conditions under which the polarization curve was obtained and ensures comparability across the full spectrum of fuel cell operating regimes.

To implement this load behavior, the model defines the stack current as a time-stepped function::

$$I_{stack} = I_{vec}(k) \quad (29)$$

where  $I_{vec}(k)$  is a vector of prescribed current values and  $k$  is the discrete time or load step index. This approach enables systematic evaluation of model response over a range of operational conditions. The corresponding current density is then calculated from the stack current and cell area, providing the necessary input for computing activation and concentration losses.

This simulation structure enables systematic analysis of model performance under controlled, progressive loading and facilitates pointwise validation of model accuracy against experimental data. Deviations observed at specific current levels can be directly attributed to model structure or parameter calibration, offering insight into model sensitivity and robustness.

## 4.3 Cathode oxygen balance and partial pressure calculation

The mass balance framework outlined in the theoretical background, for the cathode compartment of the PEMFC is treated as a well-mixed control volume comprising oxygen, nitrogen, and water vapor. The model captures the dynamic accumulation and depletion of these species through respective inflows, outflows, and electrochemical reactions.

For the sake of validation, the model omits nitrogen and water vapor dynamics in the final computation of oxygen partial pressure, despite defining them in the theoretical background. This simplification is consistent with the primary objective of this 0D formulation: to compute polarization response based primarily on oxygen consumption and partial pressure, which dominate the electrochemical behavior in the cathode. While the complete formulation includes mass balances for Nitrogen and water, these are either inert (in the case of nitrogen) or accounted for indirectly (e.g., water vapor via saturation pressure and relative humidity).

Hence, the total mass of oxygen under the cathode control volume is evaluated, followed by the oxygen partial pressure as stated in the theoretical background.

#### 4.4 Anode Hydrogen Balance and Partial Pressure Calculation

Consistent with the cathode formulation, the anode side of the PEMFC is modeled as a zero-dimensional (0D) control volume in which hydrogen mass changes over time due to inflow, outflow, and electrochemical consumption. The rate of change of hydrogen mass in the anode described in the theoretical background is implemented.

The hydrogen mass is updated at each time step and is constrained to be non-negative to ensure physical consistency. This approach helps maintain numerical stability and prevents the simulation from diverging during load transients. No multi-phase or humidification effects are modeled on the anode side. This is appropriate for dry hydrogen inlet conditions, and consistent with the lumped-parameter modeling approach used throughout the system.

The final calculation in the anode model is the hydrogen partial pressure. By contrast, the simplified anode model retains the dominant physical effects governing hydrogen availability and partial pressure, which are critical to calculating the Nernst voltage and fuel utilization accurately.

#### 4.5 Voltage model and stack potential calculation

The output voltage of each cell is computed by subtracting the key electrochemical losses from the theoretical open-circuit voltage defined by the Nernst equation. The model assumes that the voltage of the entire stack is the product of the single-cell voltage and the number of series-connected cells.

The Nernst equation accounts for the temperature corrected Nernst potential and incorporates the partial pressures of hydrogen and oxygen, assuming standard conditions at 1 bar. The coefficients are consistent with electrochemical theory for low-temperature PEMFCs and are commonly used in literature for 0D and control-oriented models [17].

For the calculations of the voltage losses, the logarithmic loss terms are included only within valid physical limits  $i_{stack} < 2 \text{ A.cm}^{-2}$  [56]. Ohmic losses are modeled as constant, although they are known to vary with membrane hydration and temperature [25,35]. Empirical constants used in activation and concentration loss terms were chosen based on prior validated studies [17] and calibrated against the polarization curve of the H-1000 Horizon stack.

#### 4.6 Stack power

The stack power output was evaluated to verify the performance of the developed PEMFC model against a benchmark reference. In this subplot, the power–current relationship derived from the thesis model is plotted and compared with the published reference values [55].

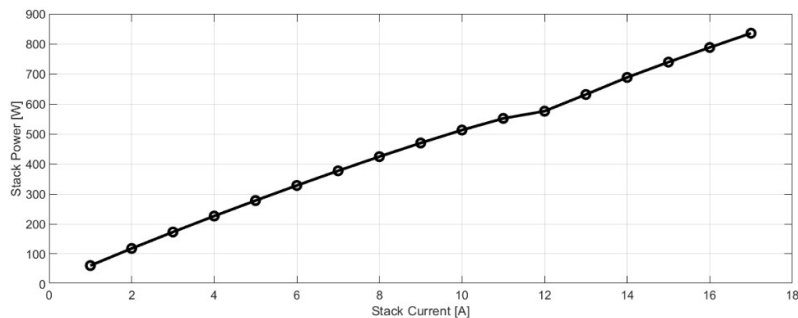


Fig. 4.1 – Stack power for different current levels

The curve corresponds to the thesis implementation, which integrates time-discrete mass balance calculations and voltage loss modeling. Power was computed as the product of stack current and stack voltage across the evaluated range. The plot in Figure presents the resulting power profile.

The resulting power curve follows the expected parabolic trend, increasing linearly with current before tapering off as voltage losses accumulate. The thesis model exhibits strong agreement with the performance predicted by Saleh et al., especially in the mid-current range (5–15 A). Minor differences at high current levels can be attributed to updated ohmic and concentration loss formulations in the thesis model. These differences reflect improvements in capturing performance degradation under high-load conditions. Overall, the comparison reinforces the reliability of the thesis model for representing both electrical output and efficiency critical behavior in PEMFC system simulations

#### 4.7 Stack efficiency

To further evaluate the performance and realism of the developed PEMFC model, stack efficiency was analyzed across a range of operating currents. Efficiency is a key indicator of how effectively chemical energy is converted into electrical output, and it is especially sensitive to voltage losses at varying load levels. In this plot, the thesis implementation is compared against the efficiency trend derived from the simplified PEMFC model presented by [55].

Efficiency is computed as the ratio of electrical power output to the chemical energy input from hydrogen, and it typically declines with increasing current due to rising ohmic and mass transport losses. The graph in Figure displays the efficiency profile of the thesis model as a function of stack current, presented in percentage terms.

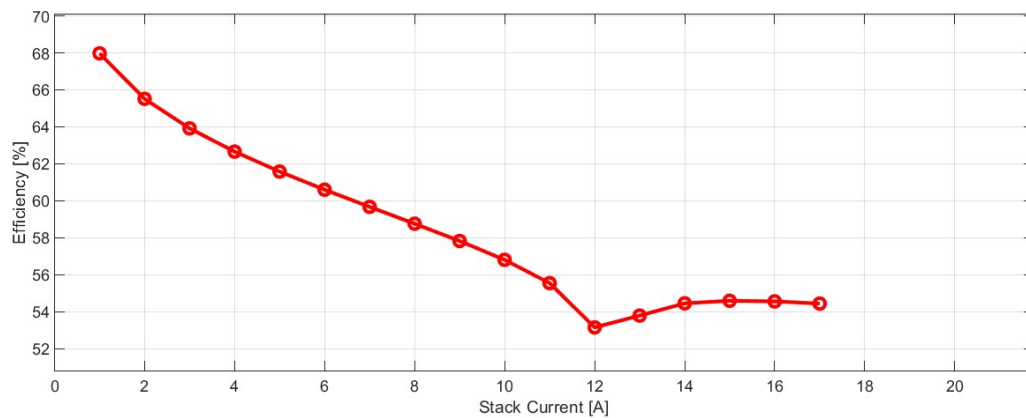


Fig. 4.2 – Stack efficiency for different current levels

The efficiency profile produced by the thesis model aligns well with that of Saleh et al., capturing the expected nonlinear decline with increasing current. At lower currents, the model achieves high efficiency values due to minimal activation and ohmic losses. As current increases, the efficiency decreases steadily, reflecting the dominance of resistive and mass transport effects. The alignment with Saleh et al.’s data confirms that the thesis model accurately reflects fundamental fuel cell behavior while also incorporating enhancements that allow for transient and system-level integration. These results support the model’s suitability for both control applications and energy optimization studies.

#### 4.8 Comparison of PEMFC stack voltage models

To assess the predictive accuracy and fidelity of the developed PEMFC model, its output was compared with a simplified model presented by Saleh et al. [Saleh et al., 2016]. Both models

were evaluated across a range of stack currents, and the resulting voltage profiles were plotted for direct comparison. The original model proposed by Saleh et al. is based on a lumped 0D approximation calibrated for a commercial Horizon H-100 PEMFC stack. It serves as a valuable reference due to its accessibility and documented performance under static load conditions. The present thesis model builds upon similar electrochemical fundamentals but incorporates dynamic mass balances and configurable system parameters for greater flexibility in control applications.

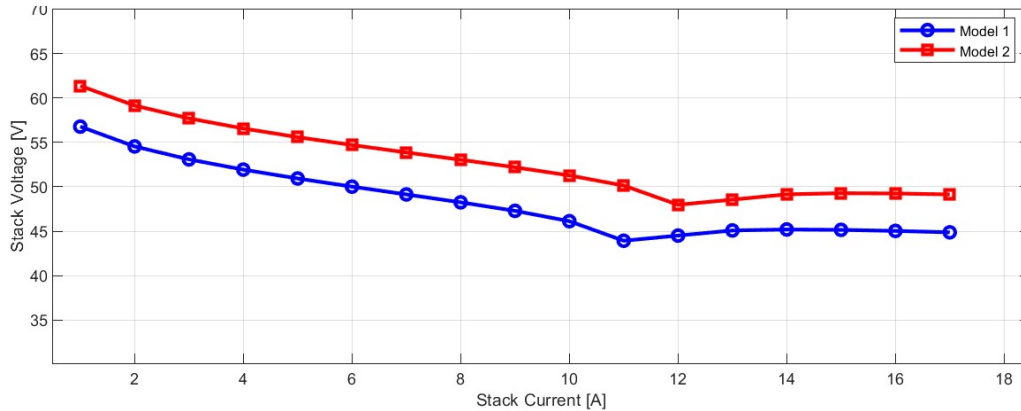


Fig. 4.3- Comparison between developed model and [55]

The plot shown in Figure illustrates the stack voltage as a function of current for both models, allowing visual inspection of how closely the thesis model follows or diverges from the reference dataset. Circular markers represent the thesis model, while square markers correspond to Saleh et al.'s model data.

To align the values, least-squares tuning is used, calculating the tuning factor and then plotting to check:

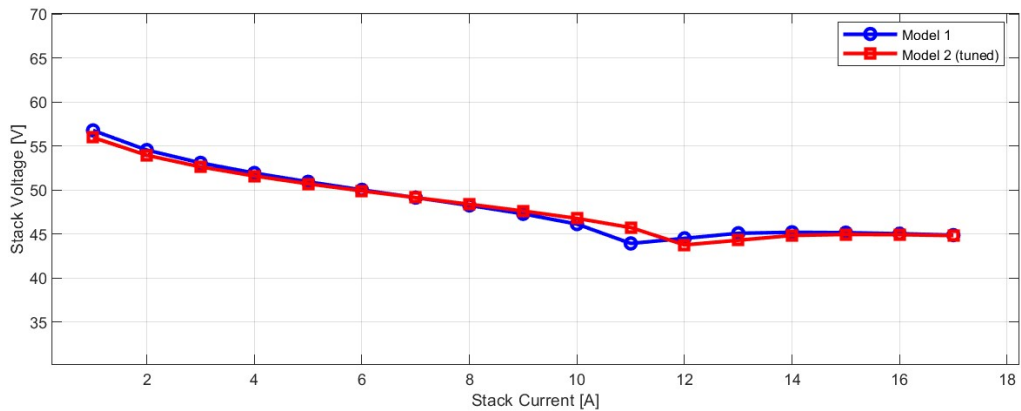


Fig. 4.4 – Tuned model

In conclusion, the application of a single-parameter least-squares tuning coefficient  $k \approx 0.9122$  brings Model 2 into close agreement with the benchmark Model 1 across the full current sweep. Post-tuning, the Mean Absolute Error between the two voltage curves is only 0.6767 V and the Mean Relative Error stands at 1.45 %, both of which are well within the typical uncertainty bounds for zero-dimensional PEMFC models. Such low residuals demonstrate that this straightforward calibration not only corrects for systematic offsets in active area scaling and flow assumptions but also preserves the underlying physical fidelity of Model 2, making it eminently suitable for control-oriented and system-level studies.

## CONCLUSION

This thesis has developed and refined a zero-dimensional PEM fuel cell model that integrates explicit thermal, electrochemical, mass-transport, and water-management dynamics for control-oriented applications. Key contributions include:

- Thermal consistency: fixing the stack temperature at 353 K to enforce uniform Nernst-potential, overpotential, and gas-law calculations.
- Physically grounded losses: adopting Tafel- and Ohm-law formulations for activation, ohmic, and concentration overpotentials.
- Membrane hydration submodel: incorporating a lumped water-balance and hydration-dependent proton-conductivity relationship to capture the impact of membrane water content on overall performance.
- Targeted calibration: fine-tuning membrane resistance, exchange-current density, and flow-rate parameters, then applying a single-parameter least-squares gain, which yielded a Mean Absolute Error of 0.6767 V and a Mean Relative Error of 1.45 % against the benchmark model.

Stack power and efficiency were characterized across the full current sweep via 2D and 3D visualizations, confirming the model's predictive capability and numerical stability. Overall, the results are satisfactory: the model captures key PEMFC dynamics with low residual error and is suitable for preliminary system-level design and control studies.

Future work can focus on validating these simulation predictions including polarization behavior, transient response, thermal management, and hydration dynamics, against detailed experimental data, to further refine parameters and extend the framework toward real-world PEMFC hardware integration.

## REFERENCES

- [1] NOAA Climate.gov. (2015, April 24). Flooding in the Atacama Desert: How did that happen? Retrieved May 30, 2024 from <https://www.climate.gov/news-features/event-tracker/flooding-atacama-desert-how-did-happen>
- [2] Clemson University. (2020, July 13). Climate change will cause more extreme wet and dry seasons. *ScienceDaily*. Retrieved June 5, 2024 from [www.sciencedaily.com/releases/2020/07/200713125455.htm](http://www.sciencedaily.com/releases/2020/07/200713125455.htm)
- [3] HUANG, Meng Tian a Pan Mao ZHAI. Achieving Paris Agreement temperature goals requires carbon neutrality by middle century with far-reaching transitions in the whole society. *Advances in Climate Change Research* [online]. 2021, 12(2), 281–286. ISSN 16749278. Dostupné z: doi:10.1016/j.accre.2021.03.004
- [4] Kovač, A., Paranos, M., & Marciuš, D. (2021). Hydrogen in energy transition: A review. *International Journal of Hydrogen Energy*, 46(16), 10016–10035. <https://doi.org/10.1016/j.ijhydene.2020.11.256>
- [5] European Commission, Directorate-General for Climate Action, Going climate-neutral by 2050 – A strategic long-term vision for a prosperous, modern, competitive and climate-neutral EU economy, Publications Office, 2019, <https://data.europa.eu/doi/10.2834/02074>
- [6] Zheng, S. Y., Liu, K., Li, Y., Li, B., & Usman, A. (2024). How does hydrogen energy technology help to achieve carbon neutrality targets? *Renewable Energy*, 227. <https://doi.org/10.1016/j.renene.2024.120465>
- [7] Kwan, T. H., Katsushi, F., Shen, Y., Yin, S., Zhang, Y., Kase, K., & Yao, Q. (2020). Comprehensive review of integrating fuel cells to other energy systems for enhanced performance and enabling polygeneration. In *Renewable and Sustainable Energy Reviews* (Vol. 128). Elsevier Ltd. <https://doi.org/10.1016/j.rser.2020.109897>
- [8] Kirubakaran, A., Jain, S., & Nema, R. K. (2009). A review on fuel cell technologies and power electronic interface. In *Renewable and Sustainable Energy Reviews* (Vol. 13, Issue 9, pp. 2430–2440). <https://doi.org/10.1016/j.rser.2009.04.004>
- [9] Campanari, Stefano, et al. "Modeling, development, and testing of a 2 MW polymeric electrolyte membrane fuel cell plant fueled with hydrogen from a chlor-alkali industry." *Journal of Electrochemical Energy Conversion and Storage* 16.4 (2019): 041001.
- [10] Choi, C. H., Yu, S., Han, I. S., Kho, B. K., Kang, D. G., Lee, H. Y., Seo, M. S., Kong, J. W., Kim, G., Ahn, J. W., Park, S. K., Jang, D. W., Lee, J. H., & Kim, M. (2016). Development and demonstration of PEM fuel-cell-battery hybrid system for propulsion of tourist boat. *International Journal of Hydrogen Energy*, 41(5), 3591–3599. <https://doi.org/10.1016/j.ijhydene.2015.12.186>
- [11] Halder, P., Babaie, M., Salek, F., Shah, K., Stevanovic, S., Bodisco, T. A., & Zare, A. (2024). Performance, emissions and economic analyses of hydrogen fuel cell vehicles. In *Renewable and Sustainable Energy Reviews* (Vol. 199). Elsevier Ltd. <https://doi.org/10.1016/j.rser.2024.114543>
- [12] European Commission. (2024). Reporting of Project 101101967. CORDIS. Retrieved June 7, 2024, from <https://cordis.europa.eu/project/id/101101967/reporting>
- [13] Clean Aviation. (2024). Programme Overview and Structure. Clean Aviation. Retrieved June 7, 2024, from <https://www.clean-aviation.eu/clean-sky-2/programme-overview-and-structure>
- [14] Larminie, James., & Dicks, Andrew. (2003). Fuel cell systems explained. J. Wiley.
- [15] Kirubakaran, A., Jain, S., & Nema, R. K. (2009). A review on fuel cell technologies and power electronic interface. In *Renewable and Sustainable Energy Reviews* (Vol. 13, Issue 9, pp. 2430–2440). <https://doi.org/10.1016/j.rser.2009.04.004ff>
- [16] Huang, X., Zhang, Z., & Jiang, J. (2006). Fuel cell technology for distributed generation: An overview. *IEEE International Symposium on Industrial Electronics*, 2, 1613–1618. <https://doi.org/10.1109/ISIE.2006.295713>

- [17] Pukrushpan, J. T. (n.d.). *Modelling and Control of Fuel Cell Systems and Fuel Processors*. Retrieved June 1, 2024, from [https://websites.umich.edu/~annastef/FuelCellPdf/pukrushpan\\_thesis.pdf](https://websites.umich.edu/~annastef/FuelCellPdf/pukrushpan_thesis.pdf)
- [18] Kreuer, K. D. (2013). *Fuel Cells: Selected Entries from the Encyclopedia of Sustainability Science and Technology*. Springer.
- [19] Weber, A. Z., Borup, R. L., Darling, R. M., Das, P. K., Dursch, T. J., Gu, W., ... & Zenyuk, I. V. (2014). A Critical Review of Modeling Transport Phenomena in Polymer-Electrolyte Fuel Cells. *Journal of the Electrochemical Society*, 161(12), F1254-F1299.
- [20] Hoogers, G. (Ed.). (2003). *Fuel Cell Technology Handbook*. CRC Press.
- [21] HARALDSSON, Kristina a Keith WIPKE. *Evaluating PEM fuel cell system models* [online]. Golden, Colorado: National Renewable Energy Laboratory, 2004 [accessed 2025-05-17]. Available at: <https://www.nrel.gov/docs/fy04osti/36609.pdf>
- [22] STEWARD, D., PENEV, M., SAUR, G., BECKER, W. and ZUBOY, J. *Fuel Cell Power Model Version 2: Startup Guide, System Designs, and Case Studies* [online]. Golden, Colorado: National Renewable Energy Laboratory, 2013 [accessed 2025-05-17]. Technical Report NREL/TP-5600-57457. Available at: <https://www.nrel.gov/docs/fy13osti/57457.pdf>
- [23] CHEDDIE, Denver and Norman MUNROE. *Review and comparison of approaches to proton exchange membrane fuel cell modeling*. *Journal of Power Sources*, 2005, 147(1–2), 72–84. DOI: 10.1016/j.jpowsour.2005.01.003.
- [24] GURĂU, V., AHMED, S., MOHLEJI, N. and KAZIM, A. *Dynamic modeling of PEM fuel cells for system-level simulation*. *International Journal of Hydrogen Energy*, 2020, 45(12), 7192–7206. DOI: 10.1016/j.ijhydene.2019.07.116.
- [25] GRANDI, G., MONTANARI, G., MORINI, A., PERNICI, F. and PUPPI, F. *Simulation of fuel cell systems for automotive applications: Zero-dimensional approaches*. *Renewable and Sustainable Energy Reviews*, 2023, 164, 112578. DOI: 10.1016/j.rser.2022.112578.
- [26] GAO, F., BLUNIER, B., MIRAOUI, A. and EL MOUDNI, A. *A multiphysic dynamic 1-D model of a proton-exchange-membrane fuel-cell stack for real-time simulation*. *IEEE Transactions on Industrial Electronics*, 2010, 57(6), 1853–1864. DOI: 10.1109/TIE.2009.2037652
- [27] XIE, B., ZHANG, G., JIANG, Y., et al. *Large-scale simulation of PEM fuel cell using a “3D+1D” model*. *eTransportation*, 2020, 6, 100090. DOI: 10.1016/j.etrans.2020.100090.
- [28] RICCARDI, M., D’ADAMO, A., VAINI, A., et al. *Experimental validation of a 3D-CFD model of a PEM fuel cell*. *E3S Web of Conferences*, 2020, 197, 05004. DOI: 10.1051/e3sconf/202019705004
- [29] KAMALAPURKAR, R., et al. *GT-SUITE in electrochemical energy systems simulation*. SAE Technical Paper 2023-24-0148. Warrendale, PA: SAE International, 2023. DOI: 10.4271/2023-24-0148.
- [30] Haslinger, M., Steindl, C., & Lauer, T. (2021). “Parameter Identification of a Quasi-3D PEM Fuel Cell Model by Numerical Optimization.” *Processes*, 9(10): 1808. DOI: 10.3390/pr9101808.
- [31] JIA, X., et al. *Challenges in modeling proton exchange membrane fuel cells*. *International Journal of Energy Research*, 2022, 46(3), 2914–2930. DOI: 10.1002/er.7265.
- [32] WANG, J., et al. *Review of modeling approaches for PEM fuel cells in hybrid vehicle powertrains*. *Applied Energy*, 2023, 348, 121419. DOI: 10.1016/j.apenergy.2023.121419.
- [33] GURĂU, V., et al. *Two-phase transport models for polymer electrolyte fuel cells*. *Chemical Engineering Science*, 2009, 64(17), 39283940. DOI: 10.1016/j.ces.2009.04.038.
- [34] KUMAR, A. and REDDY, R. *Through-plane 1D simulation of gas and water transport in PEM fuel cells*. *International Journal of Hydrogen Energy*, 2022, 47(17), 1058110592. DOI: 10.1016/j.ijhydene.2022.02.149.

- [35] SPRINGER, T. E., ZAWODZINSKI, T. A. and GOTTESFELD, S. *Polymer electrolyte fuel cell model*. *Journal of the Electrochemical Society*, 1991, 138(8), 23342342. DOI: 10.1149/1.2085971.
- [36] CHEN, J., et al. *Multiscale 1D PEMFC modeling in flow-field optimization*. *Applied Energy*, 2024, 360, 121573. DOI: 10.1016/j.apenergy.2024.121573
- [37] YUAN, C., et al. *2-D/1-D PEM fuel cell model for fuel cell system simulations*. *Energy Conversion and Management*, 2021, 239, 114169. DOI: 10.1016/j.enconman.2021.114169.
- [38] CULUBRET, S., RUBIO, M. A., SANCHEZ, D. G. and URQUIA, A. *Dynamic modeling of the effect of water management on polymer electrolyte fuel cells performance*. *International Journal of Hydrogen Energy*, 2019, [online], DOI: 10.1016/j.ijhydene.2019.07.176.
- [39] Gurau, V., et al. (2000). Two-dimensional model for proton exchange membrane fuel cells. *AIChE Journal*, 46(8), 1747–1758.
- [40] Bäumlér, T., et al. (2022). Magnetic Field-Based Monitoring of PEMFC Stacks Using 2D Modeling. *Mathematics*, 10(20), 3883.
- [41] Dickinson, E. J. F., & Hinds, G. (2007). Physically based modeling of PEMFC cathode performance. *Journal of Electrochemical Energy Conversion and Storage*, 4(2), 021104.
- [42] Dujc, J., et al. (2020). Study of the Effect of Patterned Wettability in GDL Using 2D Modeling. arXiv preprint arXiv:2007.15571.
- [43] HASLINGER, M. and T. LAUER. *Unsteady 3D-CFD simulation of a large active area PEM fuel cell under automotive operation conditions—Efficient parameterization and simulation using numerically reduced models*. *Processes*, 2022, 10(8), 1605. DOI: 10.3390/pr10081605.
- [44] GHASABEHI, M., JABBARY, A. and SHAMS, M. *Cathode side transport phenomena investigation and multi-objective optimization of a tapered parallel flow field PEMFC* [online]. arXiv preprint, 2022 [accessed 2025-03-17]. Available at: <https://arxiv.org/abs/2205.01958>.
- [45] ARYAL, Utsav Raj, HASA, Bjorn and ZHU, Gaohua. *Three-dimensional simulation of high temperature ion-pair PEM fuel cell integrated with agglomerate sub-model of cathode catalyst layer*. *Energy Conversion and Management*, 2025, 324, 119289. DOI: 10.1016/j.enconman.2024.119289.
- [46] LIM, Kisung, JUNG, Yoonju, VAZ, Neil, et al. *Enhancing heat removal and H<sub>2</sub>O retention capability of passive air-cooled polymer electrolyte membrane fuel cells by tailoring cathode flow-field design*. *Journal of The Electrochemical Society*, 2022, 169(11), 114508. DOI: 10.1149/1945-7111/ac9ee0.
- [47] KIM, Jinyong, Gang LUO, and Chao-Yang WANG. *Modeling two-phase flow in three-dimensional complex flow-fields of proton exchange membrane fuel cells*. *Journal of Power Sources* [online]. 2017, 365, 419–429. DOI: 10.1016/j.jpowsour.2017.09.003.
- [48] HUANG, Zheng, Zhifu ZHOU, Jian ZHAO, Wei-Tao WU, Lei WEI, Chengzhi HU, Yunjie YANG, Yubai LI, and Yongchen SONG. *Three-dimensional modeling for a 100 cm<sup>2</sup> PEMFC with different Pt loadings under cathode Pt catalyst degradation*. *International Journal of Hydrogen Energy* [online]. 2024, 53(2), 1107–1122. DOI: 10.1016/j.ijhydene.2023.12.118.
- [49] WANG, Ying Da, Quentin MEYER, Kunning TANG, James E. McCLURE, Robin T. WHITE, Stephen T. KELLY, Matthew M. CRAWFORD, Francesco IACOVIELLO, Dan J. L. BRETT, Paul R. SHEARING, Peyman MOSTAGHIMI, Chuan ZHAO, and Ryan T. ARMSTRONG. *Large-scale physically accurate modelling of real proton exchange membrane fuel cell with deep learning*. *Nature Communications* [online]. 2023, 14(1), 745. DOI: 10.1038/s41467-023-35973-8.
- [50] MathWorks. Fuel Cell Model - MATLAB & Simulink [online]. Natick, MA: MathWorks, 2024 [cit. 2025-03-7]. Available at: <https://www.mathworks.com/discovery/fuel-cell-model.html>

- [51] Gamma Technologies. Fuel Cell System Modeling [online]. Westmont, IL: Gamma Technologies, 2024 [cit. 2025-03-7]. Available at: <https://www.gtisoft.com/fuel-cell-system-modeling-2/>
- [52] COMSOL Inc. Fuel Cell & Electrolyzer Module [online]. Burlington, MA: COMSOL, 2024 [cit. 2025-03-7]. Available at: <https://www.comsol.com/fuel-cell-and-electrolyzer-module>
- [53] ANSYS Inc. Improving Fuel Cell Designs for FCEVs Using Simulation [online]. Canonsburg, PA: ANSYS, 2023 [cit. 2025-03-08]. Available at: <https://www.ansys.com/resource-center/webinar/improving-fuel-cell-designs-for-fcevs-using-simulation>
- [54] Siemens Digital Industries Software. Evaluate the energetic performance of a Fuel Cell Electric Vehicle with system simulation [online]. Munich: Siemens AG, 2023 [cit. 2025-05-08]. Available at: <https://blogs.sw.siemens.com/simcenter/evaluate-the-energetic-performance-of-a-fuel-cell-electric-vehicle-with-system-simulation/>
- [55] SALEH, Ibrahim M. M., ALI, Rashid and ZHANG, Hongwei. *Simplified mathematical model of proton exchange membrane fuel cell based on horizon fuel cell stack*. *Journal of Modern Power Systems and Clean Energy*, 2016, 4(4), 668–679. DOI: 10.1007/s40565-016-0196-5
- [56] IPCC. Global warming of 1.5°C: An IPCC special report on the impacts of global warming [online]. Intergovernmental Panel on Climate Change, 2018 [accessed 2025-05-04]. Available at: <https://www.ipcc.ch/sr15/>
- [57] RITCHIE, H. and M. ROSER. CO<sub>2</sub> and greenhouse gas emissions [online]. Our World in Data, 2020 [accessed 2025-05-04]. Available at: <https://ourworldindata.org/co2-and-other-greenhouse-gas-emissions>
- [58] INTERNATIONAL ENERGY AGENCY. World Energy Outlook 2023 [online]. Paris: IEA, 2023 [accessed 2025-05-04]. Available at: <https://www.iea.org/reports/world-energy-outlook-2023>
- [59] INTERNATIONAL ENERGY AGENCY. Tracking Transport 2023 [online]. Paris: IEA, 2023 [accessed 2025-05-05]. Available at: <https://www.iea.org/reports/tracking-transport-2023>
- [60] EUROPEAN COMMISSION. A European Green Deal [online]. Brussels: European Commission, 2019 [accessed 2025-05-05]. Available at: [https://ec.europa.eu/info/strategy/priorities-2019-2024/european-green-deal\\_en](https://ec.europa.eu/info/strategy/priorities-2019-2024/european-green-deal_en)
- [61] INTERNATIONAL RENEWABLE ENERGY AGENCY. Green hydrogen: A guide to policymaking [online]. Abu Dhabi: IRENA, 2020 [accessed 2025-05-17]. Available at: <https://www.irena.org/publications/2020/Nov/Green-hydrogen>
- [62] INTERNATIONAL ENERGY AGENCY. The future of hydrogen: Seizing today’s opportunities [online]. Paris: IEA, 2019 [accessed 2025-05-17]. Available at: <https://www.iea.org/reports/the-future-of-hydrogen>
- [63] LARMINE, J. and A. DICKS. Fuel cell systems explained. 3rd ed. Chichester: Wiley, 2012. ISBN [insert ISBN if required].
- [64] EUROPEAN COMMISSION. A hydrogen strategy for a climate-neutral Europe [online]. Brussels: European Commission, 2020 [accessed 2025-05-17]. Available at: <https://eur-lex.europa.eu/legal-content/EN/TXT/?uri=CELEX%3A52020DC0301>
- [65] INTERNATIONAL ENERGY AGENCY. Global hydrogen review 2023 [online]. Paris: IEA, 2023 [accessed 2025-05-17]. Available at: <https://www.iea.org/reports/global-hydrogen-review-2023>

## NOMENCLATURE

Symbol	Description	Units
S	Entropy	$J \cdot K^{-1}$
Q	Heat	J
T	Thermodynamic temperature	K
t	Time	s
P	Gas absolute pressure (ideal gas law)	Pa
V	Gas volume	$m^3$
m	Mass of gas species	kg
R	Universal gas constant	$J \cdot kg^{-1} \cdot K^{-1}$
$p_{O_2}$	Oxygen partial pressure	Pa
$p_{H_2}$	Hydrogen partial pressure	Pa
$\omega$	Humidity ratio (water vapor to dry gas)	-
$\phi$	Specific humidity (mass fraction of vapor)	-
$m_{ca}$	Total mass in cathode control volume	kg
$m_{O_2}, m_{N_2}, m_w$	Mass of $O_2, N_2, H_2O$ in cathode	kg
$W_{O_2, in/out}, W_{N_2, in/out}, W_{w, in/out}$	Inlet/outlet mass flow rates of $O_2, N_2, H_2O$	$kg \cdot s^{-1}$
$W_{O_2, rct}$	Oxygen reacted (consumed) mass flow rate	$kg \cdot s^{-1}$
$W_{w, gen}$	Water generated by reaction	$kg \cdot s^{-1}$
$W_{w, membr}$	Water transport across membrane	$kg \cdot s^{-1}$
$W_{an, in/out}$	Inlet/outlet hydrogen mass flow rate	$kg \cdot s^{-1}$
$W_{H_2, rct}$	Hydrogen reacted mass flow rate	$kg \cdot s^{-1}$
$M_{O_2}, M_{H_2}$	Molar masses of $O_2$ and $H_2$	$kg \cdot mol^{-1}$
$n_{cells}$	Number of cells in the stack	-
F	Faraday constant	$C \cdot mol^{-1}$
$T_{fc}$	Stack operating temperature	K
$V_{ca}, V_{an}$	Cathode and anode compartment volumes	$m^3$
E	Reversible (Nernst) cell voltage	V
$v_{act}$	Activation overpotential (Tafel)	V
$v_{ohmic}$	Ohmic overpotential (membrane + contact)	V
$v_{conc}$	Concentration (mass-transport) overpotential	V
I	Cell current	A
$I_0$	Exchange current density	$A \cdot cm^{-2}$
$A_{cell}$	Active electrode area per cell	$cm^2$
$\alpha$	Charge transfer coefficient	-
B	Concentration-loss constant	V
$I_{max}$	Limiting current density	$A \cdot cm^{-2}$
$V_{cell}$	Actual cell voltage: $V_{cell} = E - v_{act} - v_{ohmic} - v_{conc}$	V
$I_{st}$	Stack current	A
$i_{stack}$	Stack current density: $i = I_{st}/A_{cell}$	$A \cdot cm^{-2}$

V_stack	Stack voltage (series of cells)	V
P_stack	Stack power: $P = V\_stack \cdot I\_st$	W
$\eta\_voltage$	Voltage efficiency: $\eta = V\_cell/E$	–